A diffuse-interface approximation for surface diffusion including adatoms

2007 Nonlinearity 20 177

(http://iopscience.iop.org/0951-7715/20/1/011)

INSTITUTE OF PHYSICS PUBLISHING NONLINEARITY

Nonlinearity **20** (2007) 177–192 doi:10.1088/0951-7715/20/1/011

A diffuse-interface approximation for surface diffusion including adatoms

Andreas Rätz[1] **and A Voigt**[1,2]

[1] Crystal Growth Group, Research Center caesar, Ludwig-Erhard-Allee 2, 53175 Bonn, Germany
[2] Institut für Wissenschaftliches Rechnen, Technische Universität Dresden, 01062 Dresden, Germany

E-mail: raetz@caesar.de and voigt@caesar.de

Received 10 July 2006, in final form 21 November 2006
Published 8 December 2006
Online at stacks.iop.org/Non/20/177

Recommended by E S Titi

Abstract

We introduce a diffuse-interface approximation for solving partial differential equations on evolving surfaces. The model of interest is a fourth-order geometric evolution equation for a growing surface with an additional diffusive adatom density on the surface. Such models arise in the description of epitaxial growth, where the surface of interest is the solid–vapour interface. The model allows us to handle complex geometries in an implicit manner, by considering an evolution equation for a phase-field variable describing the surface and an evolution equation for an extended adatom concentration on a time-independent domain. Matched asymptotic analysis shows the formal convergence towards the sharp interface model and numerical results based on adaptive finite elements demonstrate the applicability of the approach.

Mathematics Subject Classification: 35K55, 35K65, 37E35

(Some figures in this article are in colour only in the electronic version)

1. Introduction

Partial differential equations on evolving surfaces can be found in a wide range of applications, e.g. in materials science, biophysics or image processing[3]. A conservation equation of a scalar

[3] The basic geometric object here is an evolving embedded d-dimensional surface $\Gamma = \Gamma(t) \subset \mathbb{R}^{d+1}$ during a time interval $t \in [0, T]$, $T > 0$. Denoting the principle curvatures by κ_i we thereby consider the mean curvature $H = \nabla_\Gamma \cdot \boldsymbol{n} = \sum_{i=1}^{d} \kappa_i$ and the normal $\boldsymbol{n}$ of the surface, where we use for closed surfaces the sign convention that $\boldsymbol{n}$ is the outer normal and H is positive if the domain surrounded by Γ is convex. If the surface is given by the graph of a function f with $f : G \subset \mathbb{R}^d \to \mathbb{R}$, we assume that $H > 0$ for concave functions f and $\boldsymbol{n}$ points into the positive f-direction for $f = \text{const}$.

function $u : [0, T] \times \Gamma$ on an evolving surface $\Gamma(t)$, with zero tangential velocity, reads

$$\overset{\square}{u} + uHV = -\nabla_\Gamma \cdot \boldsymbol{q} \qquad \text{on } \Gamma(t) \tag{1}$$

with the normal velocity V of the surface, ∇_Γ the surface divergence, $\boldsymbol{q}$ the surface flux and $\overset{\square}{u}$ the normal time-derivative, see, e.g. [7]. The surface flux typically depends on the evolution and V is typically determined by a geometric evolution equation, which might depend on the scalar quantity u. If we denote the normally constant extension of u by $\hat{u}$ equation (1) is equivalent to

$$\partial_t \hat{u} + \hat{u} H V = -\nabla_\Gamma \cdot \hat{\boldsymbol{q}} \qquad \text{on } \Gamma(t). \tag{2}$$

For convenience we will drop the $\hat{}$ in the following and always work with normally constant extensions. Numerical approaches for such problems have been introduced in the level set context [1, 20] and within a parametric setting [8]. However, in both approaches the velocity V is a given quantity.

In this paper we propose a phase-field approximation [4] for problems involving (1) or (2), where the velocity V is implicitly determined through the solution of a partial differential equation. A phase-field approximation for evolution equations on stationary surfaces ($V = 0$) has recently been proposed [16]. This work is now extended to evolving surfaces by approximating the additional term uHV within the phase-field context. The corresponding phase-field representation to (1) or (2) on the time-independent domain Ω, with $\Gamma(t) \subset \Omega$, reads

$$\left(\frac{\epsilon}{2}|\nabla\phi|^2 + \frac{1}{\epsilon}G(\phi)\right)\partial_t u + \left(-\epsilon\nabla\cdot(u\nabla\phi) + \frac{1}{\epsilon}G'(\phi)u\right)\partial_t\phi = -\frac{1}{\epsilon}\nabla\cdot(B(\phi)\boldsymbol{q}) \qquad \text{on } \Omega \tag{3}$$

with ϕ being a phase-field variable, implicitly determining the evolving surface $\Gamma(t)$, u the extended scalar quantity, $G(\phi)$ a double-well potential, $B(\phi)$ a mobility function which restricts the evolution to the diffuse interface, $\boldsymbol{q}$ the extended surface flux and $\epsilon > 0$ a small parameter determining the width of the diffuse interface. The correspondence between (1) and (3) can heuristically be seen as follows:

(a) the term $\frac{\epsilon}{2}|\nabla\phi|^2 + \frac{1}{\epsilon}G(\phi)$ is zero away from the diffuse interface; thus the first term in (3) approximates the first term in (1),
(b) $-\epsilon\Delta\phi + \frac{1}{\epsilon}G'(\phi)$ is an approximation for H and thus $(-\epsilon\nabla\cdot(u\nabla\phi) + \frac{1}{\epsilon}G'(\phi)u)$ is an approximation for uH; furthermore $\partial_t\phi$ is an approximation for V; thus the second term in (3) approximates the second term in (1),
(c) $B(\phi)$ is zero away from the diffuse interface; thus the evolution is restricted to the diffuse interface and the third term in (3) approximates the third term in (1).

Equation (3) is coupled to an evolution equation for ϕ, which is a diffuse-interface approximation of the geometric evolution law determining V and might depend on u.

We derive the phase-field model for a prototype example from materials science. In the example the partial differential equation on the surface is of the diffusion type and the surface evolves by mean curvature flow.

[4] Much progress in the understanding of pattern formation on mesoscopic scales is associated with the development of phase-field models. These phase-field models use a time- and space-dependent variable ϕ to describe the thermodynamic state of the system. In the field of solidification such models are today the model of choice [3]. Here the solid phase corresponds to $\phi = 1$ and the liquid phase to $\phi = 0$. The interface between the phases is identified by a smooth but highly localized transition between 1 and 0. From a theoretical viewpoint the phase-field approach has the advantage in providing a unified description of the system, in which the set of governing equations in the bulk and for the interface regions can be derived at the same time in a thermodynamically consistent way. From a numerical point of view, the continuous model avoids the explicit tracking of the interface and naturally allows for topological changes during the evolution.

1.1. Surface evolution models for epitaxial growth

One approach to describe the evolving surface follows from a geometric description. Considering a continuous surface, we can derive evolution laws for its normal velocity V. Such models typically read $V = -\nabla_\Gamma \cdot \boldsymbol{j} - \boldsymbol{F} \cdot \boldsymbol{n}$, with ∇_Γ the surface divergence, $\boldsymbol{j}$ the surface current and $\boldsymbol{F}$ the deposition flux. If $\boldsymbol{j} = -\nabla_\Gamma \mu$, with μ the surface chemical potential, defined as the variational derivative of the surface free energy, with respect to surface variations, and ∇_Γ the surface gradient, the resulting equation is the model for surface diffusion [13]. In the case of $\mu = H$ and $\boldsymbol{F} = 0$, we obtain the standard isotropic surface diffusion equation

$$V = \Delta_\Gamma H, \tag{4}$$

with Δ_Γ the surface Laplacian. A more general geometric evolution law which accounts also for kinetic effects besides the surface diffusion [6, 10] reads

$$V = \Delta_\Gamma \mu - \boldsymbol{F} \cdot \boldsymbol{n}, \tag{5}$$

$$bV + H - \mu = 0, \tag{6}$$

with b a positive kinetic coefficient. The kinetic term bV models a dissipative force, which is associated with the rearrangement of atoms on the solid surface.

Both models do not consider the actual objects which lead to the modification of the surface, namely the free adatoms on it. They attach and detach at surface defects and thereby evolve the surface. Only recently a model which accounts for adatoms in the evolution has been proposed [10]

$$\partial_t u + V + uHV = \Delta_\Gamma \mu - \boldsymbol{F} \cdot \boldsymbol{n}, \tag{7}$$

$$bV + \psi H - \mu - uH\mu = 0, \tag{8}$$

with u the adatom concentration[5]. The chemical potential μ is now defined as

$$\mu = \psi'(u), \tag{11}$$

with ψ the surface free energy density. Here we assume zero tangential velocity as in [4], which corresponds to neglecting elastic effects in the more general treatment in [10].

The advantages of a phase-field model described above can be carried over to other problems. In the field of epitaxial growth phase-field models have been used in [15, 19]. An appropriate mobility function is needed in these models to account for the different mass transport mechanisms compared with solidification, in which the attachment–detachment processes dominate. The surface diffusion mechanisms in epitaxial growth are modelled by restricting the evolution of the phase-field to the diffuse-interface region, which leads to degenerate equations.

1.2. Adatom diffusion model

For simplicity we will consider in the following a prototype free energy density of the form $\psi(u) = 1 + u^2/2$. Thus the equations read

$$\partial_t u + V + uHV = \Delta_\Gamma u - \boldsymbol{F} \cdot \boldsymbol{n}, \tag{12}$$

$$bV + H - u - \frac{1}{2}u^2 H = 0. \tag{13}$$

[5] The model is written in a dimensionless form. A version of (7) and (8) in physical units includes the bulk density ρ and a diffusion coefficient L and reads

$$\partial_t u + \rho V + uHV = \nabla_\Gamma \cdot (L \nabla_\Gamma \mu) - \boldsymbol{F} \cdot \boldsymbol{n}, \tag{9}$$

$$bV + \psi H - \rho\mu - uH\mu = 0, \tag{10}$$

where we have used the same notations for dimensional quantities as for the dimensionless ones in (7) and (8).

The model is derived in [10] within the framework of configurational forces. In [4] the model is analysed in detail and numerically solved in a graph formulation. While generally considered negligible in surface evolution models and assumed to play an important role only for segregation of various atomic species, a remarkable modification of the evolution path towards the equilibrium shape has numerically been observed in [4] if adatoms are present. These results are the physical motivation for our study. However, besides its physical relevance, the parabolic nature of the equations if adatoms are present might regularize the overall system of equations and might therefore help to solve the evolution equations efficiently.

1.3. Paper outline

The outline of the paper is as follows: in section 2 we derive the phase-field model from an appropriate free energy and show the thermodynamic consistency of the model. In section 3 we prove by matched asymptotic analysis the convergence of the phase-field approximation towards equation (12) and (13). In section 4 we discuss a numerical approach by adaptive finite elements. In section 5 we show several simulation results and in section 6 we finally draw conclusions.

2. Model derivation

To derive a phase-field model for the adatom surface diffusion model the approach in [16] needs to be extended to evolving surfaces. The basic ingredients to derive the model are an appropriate free energy and mass conservation.

2.1. Thermodynamically consistent model

We start with a free energy, defined over the time-independent domain Ω, such that the surface $\Gamma(t) \subset \Omega$, of the form

$$E[\phi, u] = \int_\Omega \left(\frac{\epsilon}{2}|\nabla\phi|^2 + \frac{1}{\epsilon}G(\phi)\right)\left(1 + \frac{1}{2}u^2\right) \mathrm{d}x \tag{14}$$

with ϕ being a phase-field variable, u the extended adatom concentration, $G(\phi)$ a double-well potential, defined as

$$G(\phi) = 18\phi^2(1-\phi)^2, \tag{15}$$

and $\epsilon > 0$ a small parameter, determining the interfacial thickness. The phase-field variable is approximately 1 in the film, 0 outside and is smoothly varying between 0 and 1 within the diffuse-interface region. Note that for $u = 0$ equation (14) is the usual Ginzburg–Landau energy approximating the area functional of the interface Γ. We first compute the variational derivatives of E with respect to ϕ and u

$$\frac{\delta E}{\delta \phi} = -\epsilon\Delta\phi + \frac{1}{\epsilon}G'(\phi) - \frac{\epsilon}{2}\nabla\cdot(u^2\nabla\phi) + \frac{1}{2\epsilon}u^2G'(\phi), \tag{16}$$

$$\frac{\delta E}{\delta u} = \left(\frac{\epsilon}{2}|\nabla\phi|^2 + \frac{1}{\epsilon}G(\phi)\right)u. \tag{17}$$

The mass in the system is defined through the contribution from the species in the bulk and the species on the surface and is given by[6]

$$m_\epsilon(t) = \int_\Omega \phi \,\mathrm{d}x + \int_\Omega \left(\frac{\epsilon}{2}|\nabla\phi|^2 + \frac{1}{\epsilon}G(\phi)\right) u \,\mathrm{d}x. \tag{18}$$

The first term is the mass in the bulk, with the density in the bulk assumed to be 1. The second term is the mass on the surface. Through the 'area element' $\frac{\epsilon}{2}|\nabla\phi|^2 + \frac{1}{\epsilon}G(\phi)$ we restrict this term to the diffuse interface and thus measure the density u only within this region, because $\nabla\phi$ as well as $G(\phi)$ vanish outside the diffuse interface. We now choose for given $t \in [0, T]$ an arbitrary time-independent domain $\Sigma \subset \Omega$, such that $\Sigma \cap \Gamma(t) \neq \emptyset$. In order to establish mass conservation we need

$$\frac{\mathrm{d}}{\mathrm{d}t} m_\epsilon(t)_{|\Sigma} = \frac{\mathrm{d}}{\mathrm{d}t}\left(\int_\Sigma \phi \,\mathrm{d}x + \int_\Sigma \left(\frac{\epsilon}{2}|\nabla\phi|^2 + \frac{1}{\epsilon}G(\phi)\right) u \mathrm{d}\, x\right) = -\int_{\partial\Sigma} \boldsymbol{j}\cdot\boldsymbol{m}\,\mathrm{d}s \tag{19}$$

with $\boldsymbol{j}$ the material flux and $\boldsymbol{m}$ the normal onto $\partial\Sigma$. Then we obtain

$$\int_\Sigma \partial_t\phi \,\mathrm{d}x + \int_\Sigma \left(\frac{\epsilon}{2}|\nabla\phi|^2 + \frac{1}{\epsilon}G(\phi)\right)\partial_t u \,\mathrm{d}x + \int_\Sigma \left(\epsilon\nabla\phi\cdot\nabla\partial_t\phi + \frac{1}{\epsilon}G'(\phi)\partial_t\phi\right) u \,\mathrm{d}x$$
$$= -\int_\Sigma \nabla\cdot\boldsymbol{j}\,\mathrm{d}x$$

and thus

$$\partial_t\phi + \left(\frac{\epsilon}{2}|\nabla\phi|^2 + \frac{1}{\epsilon}G(\phi)\right)\partial_t u + \epsilon u\nabla\phi\cdot\nabla\partial_t\phi + \frac{1}{\epsilon}G'(\phi)u\partial_t\phi = -\nabla\cdot\boldsymbol{j}. \tag{20}$$

By (17) we thus obtain

$$\partial_t u\frac{\delta E}{\delta u} = -u\partial_t\phi - \epsilon u^2\nabla\phi\cdot\nabla\partial_t\phi - \frac{1}{\epsilon}G'(\phi)u^2\partial_t\phi - u\nabla\cdot\boldsymbol{j},$$

and by

$$\frac{\mathrm{d}}{\mathrm{d}t}E[\phi, u] = \int_\Omega \partial_t\phi\frac{\delta E}{\delta\phi}\,\mathrm{d}x + \int_\Omega \partial_t u\frac{\delta E}{\delta u}\,\mathrm{d}x \tag{21}$$

we obtain

$$\frac{\mathrm{d}}{\mathrm{d}t}E[\phi, u] = \int_\Omega \partial_t\phi\frac{\delta E}{\delta\phi}\,\mathrm{d}x + \int_\Omega -u\partial_t\phi - \epsilon u^2\nabla\phi\cdot\nabla\partial_t\phi - \frac{1}{\epsilon}G'(\phi)u^2\partial_t\phi - u\nabla\cdot\boldsymbol{j}\,\mathrm{d}x.$$

We now define

$$\boldsymbol{j} := -\frac{1}{\epsilon}B(\phi)\nabla u - \epsilon u\partial_t\phi\nabla\phi \tag{22}$$

with $B(\phi) = 6\phi(1-\phi)$ an appropriate mobility function[7], which yields

$$\frac{\mathrm{d}}{\mathrm{d}t}E[\phi, u] = \int_\Omega \partial_t\phi\left(\frac{\delta E}{\delta\phi} - u + u\left(\epsilon\nabla\cdot(u\nabla\phi) - \frac{1}{\epsilon}G'(\phi)u\right)\right)\mathrm{d}x - \frac{1}{\epsilon}\int_\Omega B(\phi)\nabla u\cdot\nabla u\,\mathrm{d}x.$$

Furthermore we define

$$\epsilon b\partial_t\phi := -\frac{\delta E}{\delta\phi} + u - u\left(\epsilon\nabla\cdot(u\nabla\phi) - \frac{1}{\epsilon}G'(\phi)u\right),$$

[6] In physical units (18) reads (again using the same notations for dimensional and dimensionless quantities)

$$m_\epsilon(t) = \int_\Omega \rho\phi\,\mathrm{d}x + \int_\Omega \left(\frac{\epsilon}{2}|\nabla\phi|^2 + \frac{1}{\epsilon}G(\phi)\right) u\,\mathrm{d}x$$

and leads to an appropriate diffuse interface approximation of the sharp interface model in physical units (9), (10).

[7] For the approximation of the model in physical units (9), (10) one defines $B(\phi) = 6L\phi(1-\phi)$.

which guarantees thermodynamic consistency

$$\frac{\mathrm{d}}{\mathrm{d}t}E[\phi,u]\leqslant 0.$$

Using (16) and the chain rule we thus obtain

$$\begin{aligned}\epsilon b\partial_t\phi &= \epsilon\Delta\phi-\frac{1}{\epsilon}G'(\phi)+\frac{\epsilon}{2}\nabla\cdot(u^2\nabla\phi)-\frac{1}{2\epsilon}u^2G'(\phi)+u-u\left(\epsilon\nabla\cdot(u\nabla\phi)-\frac{1}{\epsilon}G'(\phi)u\right)\\ &= \epsilon\Delta\phi-\frac{1}{\epsilon}G'(\phi)+\epsilon u\nabla u\cdot\nabla\phi+\frac{\epsilon}{2}u^2\Delta\phi+u-\epsilon u\nabla u\cdot\nabla\phi-\epsilon u^2\Delta\phi+\frac{1}{2\epsilon}u^2G'(\phi)\\ &= \epsilon\Delta\phi-\frac{1}{\epsilon}G'(\phi)+u-\frac{\epsilon}{2}u^2\Delta\phi+\frac{1}{2\epsilon}u^2G'(\phi)\\ &= \left(\epsilon\Delta\phi-\frac{1}{\epsilon}G'(\phi)\right)\left(1-\frac{1}{2}u^2\right)+u.\end{aligned}$$

The governing equations for u and ϕ now read

$$\left(\frac{\epsilon}{2}|\nabla\phi|^2+\frac{1}{\epsilon}G(\phi)\right)\partial_t u+\left(-\epsilon\nabla\cdot(u\nabla\phi)+\frac{1}{\epsilon}G'(\phi)u\right)\partial_t\phi+\partial_t\phi=\frac{1}{\epsilon}\nabla\cdot(B(\phi)\nabla u),\quad(23)$$

$$\epsilon b\partial_t\phi-\left(\epsilon\Delta\phi-\frac{1}{\epsilon}G'(\phi)\right)\left(1-\frac{1}{2}u^2\right)-u=0.\quad(24)$$

Equation (23) can be viewed as a phase-field approximation for a diffusion equation for u on an evolving surface. Comparing the equation with the approximation for a diffusion equation on a fixed surface, introduced in [16], only the second and third terms on the left-hand side differ. They account for the evolution and vanish if $\partial_t\phi=0$, which corresponds to a fixed surface. Equation (24) can be viewed as an Allen–Cahn type equation determining the evolution for ϕ. The only difference are the terms entering according to u.

Remark 1. *Equation (23) can be generalized to serve as a general phase-field approximation for any evolution equation on an evolving surface with zero tangential velocity. The equation on Ω reads*

$$\left(\frac{\epsilon}{2}|\nabla\phi|^2+\frac{1}{\epsilon}G(\phi)\right)\partial_t u+\left(-\epsilon\nabla\cdot(u\nabla\phi)+\frac{1}{\epsilon}G'(\phi)u\right)\partial_t\phi=-\frac{1}{\epsilon}\nabla\cdot(B(\phi)\boldsymbol{q})\quad(25)$$

with $\phi(\boldsymbol{x},t)$ an appropriate phase-field variable specifying the normal evolution of the surface and $u(\boldsymbol{x},t)$ and $\boldsymbol{q}(\boldsymbol{x},t)$ the extended interfacial quantities. The corresponding sharp interface model on $\Gamma(t)$ reads

$$\partial_t u+uHV=-\nabla_\Gamma\cdot\boldsymbol{q}.\quad(26)$$

2.2. Incorporation of deposition flux

The deposition flux can be added as in [9,15]. We need to restrict the deposition to the diffuse interface which can be done by adding

$$-\frac{1}{\epsilon}\boldsymbol{F}_\phi\cdot\boldsymbol{n}_\phi=\frac{1}{\epsilon}B(\phi)\boldsymbol{F}\cdot\frac{\nabla\phi}{|\nabla\phi|}\quad(27)$$

to the right-hand side of equation (23), where $\boldsymbol{F}_\phi := B(\phi)\boldsymbol{F}$ and $\boldsymbol{n}_\phi := -\nabla\phi/|\nabla\phi|$. This yields

$$\left(\frac{\epsilon}{2}|\nabla\phi|^2 + \frac{1}{\epsilon}G(\phi)\right)\partial_t u + \left(-\epsilon\nabla\cdot(u\nabla\phi) + \frac{1}{\epsilon}G'(\phi)u\right)\partial_t\phi + \partial_t\phi$$
$$= \frac{1}{\epsilon}\nabla\cdot(B(\phi)\nabla u) + \frac{1}{\epsilon}B(\phi)\boldsymbol{F}\cdot\frac{\nabla\phi}{|\nabla\phi|}, \tag{28}$$

$$\epsilon b\partial_t\phi - \left(\epsilon\Delta\phi - \frac{1}{\epsilon}G'(\phi)\right)\left(1 - \frac{1}{2}u^2\right) - u = 0. \tag{29}$$

3. Asymptotic expansion

We now provide a matched asymptotic analysis (see, e.g. [5, 14]) to show the formal convergence of (28), (29) to (12), (13) as $\epsilon \to 0$.

3.1. New coordinates

New coordinates are established in a neighbourhood of the interface Γ. To this end $r = r(x,t;\epsilon)$ is defined as the signed distance of x from $\Gamma(t)$ being positive in the region specified through $\phi < 0$. Furthermore let $\boldsymbol{X} : S \times [0,T] \to \mathbb{R}^{d+1}$ be a parametric representation of Γ, where S is an oriented surface of dimension d. Let $\boldsymbol{n} = \boldsymbol{n}(s,t;\epsilon)$, $s \in S$, denote the normal. Then we assume that for $0 < \rho \ll 1$ there exists a neighbourhood

$$U_\epsilon = \{(x) \in \Omega : |r(x,t;\epsilon)| < \rho\} \tag{30}$$

of Γ_ϵ such that one can write $x = \boldsymbol{X}(s,t;\epsilon) + r(x,t;\epsilon)\boldsymbol{n}(s,t;\epsilon)$ for $x \in U_\epsilon$. Now one transforms u and ϕ to the new coordinate system:

$$\hat{u}(r,s,t;\epsilon) := u(\boldsymbol{X}(s,t;\epsilon) + r\boldsymbol{n}(s,t;\epsilon),t;\epsilon), \qquad x \in U_\epsilon,$$
$$\hat{\phi}(r,s,t;\epsilon) := \phi(\boldsymbol{X}(s,t;\epsilon) + r\boldsymbol{n}(s,t;\epsilon),t;\epsilon), \qquad x \in U_\epsilon.$$

Furthermore, a stretched variable is introduced, $z := \frac{r}{\epsilon}$, and one defines

$$U(z,s,t;\epsilon) := \hat{u}(r,s,t;\epsilon),$$
$$\Phi(z,s,t;\epsilon) := \hat{\phi}(r,s,t;\epsilon).$$

In addition, the following Taylor expansion approximations for small ϵ are assumed to be valid

$$u(x,t;\epsilon) = u_0(x,t) + \mathcal{O}(\epsilon), \tag{31}$$
$$\hat{u}(r,s,t;\epsilon) = \hat{u}_0(r,s,t) + \mathcal{O}(\epsilon), \tag{32}$$
$$U(z,s,t;\epsilon) = U_0(z,s,t) + \epsilon U_1(z,s,t) + \epsilon^2 U_2(z,s,t) + \mathcal{O}(\epsilon^3), \tag{33}$$
$$\phi(x,t;\epsilon) = \phi_0(x,t) + \mathcal{O}(\epsilon), \tag{34}$$
$$\hat{\phi}(r,s,t;\epsilon) = \hat{\phi}_0(r,s,t) + \mathcal{O}(\epsilon), \tag{35}$$
$$\Phi(z,s,t;\epsilon) = \Phi_0(z,s,t) + \epsilon\Phi_1(z,s,t) + \mathcal{O}(\epsilon^2), \tag{36}$$

for which (31), (32) and (34), (35) are called outer expansions while (33), (36) are called inner expansions. It is assumed that these hold simultaneously in some overlapping region and represent the same functions, which yields the matching conditions

$$\lim_{r\to\pm 0}\hat{u}_0(r,s,t) = \lim_{z\to\pm\infty}U_0(z,s,t), \tag{37}$$

$$\lim_{r\to\pm 0}\hat{\phi}_0(r,s,t) = \lim_{z\to\pm\infty}\Phi_0(z,s,t). \tag{38}$$

Let $H = H(s,t;\epsilon) = \sum_{i=1}^{d} \kappa_i$ denote the mean curvature of Γ with the principal curvatures κ_i. The transform of the derivatives into the new coordinates (z,s) lead to

$$\nabla u = \epsilon^{-1}\partial_z U \boldsymbol{n} + \sum_{i,j=1}^{2} g^{ij}\partial_{s_i} U \partial_{s_j}\boldsymbol{X} + \mathcal{O}(\epsilon), \tag{39}$$

$$\Delta u = \epsilon^{-2}\partial_z^2 U + \epsilon^{-1} H \partial_z U + \Delta_\Gamma U + \mathcal{O}(\epsilon), \tag{40}$$

$$\partial_t u = -\epsilon^{-1} v \partial_z U + \partial_t U + \mathcal{O}(\epsilon), \tag{41}$$

where $g_{ij} := \boldsymbol{X}_{s_i} \cdot \boldsymbol{X}_{s_j}$ and $(g^{ij}) := (g_{ij})^{-1}$. We will need the formula

$$\nabla \cdot (B(\phi)\nabla u) = \epsilon^{-2}\partial_z(B(\Phi)\partial_z U) + B(\Phi)(\epsilon^{-1} H \partial_z U + \Delta_\Gamma U) + \mathcal{O}(\epsilon) \tag{42}$$

as well as (see [15])

$$-\frac{\nabla\phi}{|\nabla\phi|} = \boldsymbol{n} + \mathcal{O}(\epsilon). \tag{43}$$

3.2. *Outer expansion*

By inserting the outer expansions into (29) and assuming $u_0(x,0) < \sqrt{2}\ \forall x$ we obtain

$$G'(\phi_0) = 0 \Rightarrow \phi_0 \in \{0,1\}, \tag{44}$$

and

$$\lim_{r\to+0} \phi_0 = 0, \qquad \lim_{r\to-0} \phi_0 = 1. \tag{45}$$

3.3. *Inner expansion*

First we insert the inner expansion (36) in (29) and get in $\mathcal{O}(\epsilon^{-1})$

$$\partial_z^2 \Phi_0 - G'(\Phi_0) = 0. \tag{46}$$

From this one gets

$$\partial_z \Phi_0 = -\sqrt{2G(\Phi_0)} \tag{47}$$

as well as by definition of G (see equation (15))

$$\int_{-\infty}^{+\infty} (\partial_z \Phi_0)^2 \,\mathrm{d}z = \int_0^1 \sqrt{2G(\phi)}\,\mathrm{d}\phi = 1. \tag{48}$$

Because $\Phi_0(0) = 1/2$ and $\partial_z\Phi_0(0) = -\sqrt{2G(\Phi_0)(0)} = -3/2$ as well as (46) are independent of s_i and t one arrives at

$$\partial_{s_i}\Phi_0 = \partial_t \Phi_0 = 0. \tag{49}$$

Using (42) in (28) we obtain in $\mathcal{O}(\epsilon^{-3})$

$$\partial_z(B(\Phi_0)\partial_z U_0) = 0,$$

which yields $\partial_z U_0 = 0$. From this one gets in $\mathcal{O}(\epsilon^{-2})$

$$\partial_z(B(\Phi_0)\partial_z U_1) = -V\partial_z\Phi_0(\partial_z(U_0\partial_z\Phi_0) - G'(\Phi_0)U_0) = 0$$

and therefore $\partial_z U_1 = 0$. And finally we have in $\mathcal{O}(\epsilon^{-1})$

$$\left(\frac{1}{2}(\partial_z\Phi_0)^2 + G(\Phi_0)\right)\partial_t U_0 + U_0\left(\partial_z^2\Phi_1 - G''(\Phi_0)\Phi_1\right) V\partial_z\Phi_0 + V H U_0(\partial_z\Phi_0)^2 - V\partial_z\Phi_0$$
$$= \partial_z(B(\Phi_0))\partial_z U_2) + B(\Phi_0)\Delta_\Gamma U_0 - B(\Phi_0)\boldsymbol{F}\cdot\boldsymbol{n}. \tag{50}$$

Furthermore we use (47) and (48), and integration of (50) yields

$$\partial_t U_0 + V H U_0 + V = \int_{-\infty}^{+\infty} B(\Phi_0)\,\mathrm{d}z\,\Delta_\Gamma U_0 - \int_{-\infty}^{+\infty} B(\Phi_0)\,\mathrm{d}z \boldsymbol{F}\cdot\boldsymbol{n}.$$

By the choice of B one has

$$\int_{-\infty}^{+\infty} B(\Phi_0)\,\mathrm{d}z = 1,$$

and we end up with

$$\partial_t U_0 + V H U_0 + V = \Delta_\Gamma U_0 - \boldsymbol{F}\cdot\boldsymbol{n}.$$

Thus with $\lim_{z\to\pm\infty} U_0 = \lim_{r\to\pm 0} u_0 = u_0|_\Gamma$ we have shown the formal convergence to the diffusion equation (12) on the surface Γ.

Now we again consider (29) and obtain in $\mathcal{O}(\epsilon^0)$

$$-bV\partial_z\Phi_0 - \left(\partial_z^2\Phi_1 - G''(\Phi_0)\Phi_1\right)\left(1-\tfrac{1}{2}U_0^2\right) - H\left(1-\tfrac{1}{2}U_0^2\right)\partial_z\Phi_0 - U_0 = 0. \tag{51}$$

Testing (51) with $\partial_z\Phi_0$ one arrives at

$$bV + H\left(1-\tfrac{1}{2}U_0^2\right) - U_0 = 0,$$

which yields the desired evolution equation (13).

To provide a rigorous proof of this formally derived result one would have to apply the techniques of [2].

4. Discretization

We use a finite element approach to discretize the system of equations. The weak form for (28) and (29) reads

$$\int_\Omega \left(\frac{\epsilon}{2}|\nabla\phi|^2 + \frac{1}{\epsilon}G(\phi)\right)\partial_t u\eta\,\mathrm{d}x + \int_\Omega \epsilon u\nabla\phi\cdot\nabla\partial_t\phi\eta\,\mathrm{d}x + \int_\Omega \epsilon u\nabla\phi\cdot\nabla\eta\partial_t\phi\,\mathrm{d}x$$
$$+ \int_\Omega \frac{1}{\epsilon}B(\phi)\nabla u\cdot\nabla\eta\,\mathrm{d}x + \int_\Omega \frac{1}{\epsilon}uG'(\phi)\partial_t\phi\eta\,\mathrm{d}x + \int_\Omega \partial_t\phi\eta\,\mathrm{d}x = \int_\Omega \frac{1}{\epsilon}\boldsymbol{F}\cdot\frac{\nabla\phi}{|\nabla\phi|}B(\phi)\eta\,\mathrm{d}x,$$

$$\int_\Omega \epsilon b\partial_t\phi\eta\,\mathrm{d}x + \int_\Omega \epsilon(1-\frac{1}{2}u^2)\nabla\phi\cdot\nabla\eta\,\mathrm{d}x - \int_\Omega \epsilon\nabla\phi\cdot\nabla u u\eta\,\mathrm{d}x + \int_\Omega \frac{1}{\epsilon}G'(\phi)\left(1-\frac{1}{2}u^2\right)\eta\,\mathrm{d}x$$
$$- \int_\Omega u\eta\,\mathrm{d}x = 0,$$

with appropriate test functions η. Discretization of the system by a fully implicit scheme would lead to an expensive method, because a highly nonlinear system has to be solved in each time step. Fully explicit methods on the other hand are also ruled out because of the severe time step restrictions for higher order equations. To improve the stability and accuracy of the approximations in time while maintaining comparable efficiency, we therefore apply a semi-implicit time discretization, with the aim of treating the highest order derivatives implicit.

4.1. Operator splitting

To discretize in time we use an operator splitting approach for the two equations and start with the second to obtain ϕ^{n+1} by given ϕ^n and u^n. The time interval is split by discrete time instants $0 = t_0 < t_1 < \cdots$, from which we obtain the time steps $\tau^n = t_{n+1} - t_n$, $n = 0, 1, \ldots$.

We use a semi-implicit time discretization, in which the nonlinear term $G'(\phi^{n+1})$ is linearized around ϕ^n:

$$\int_\Omega \epsilon b \frac{\phi^{n+1}-\phi^n}{\tau^n}\eta\,\mathrm{d}x + \int_\Omega \epsilon\left(1-\frac{1}{2}(u^n)^2\right)\nabla\phi^{n+1}\cdot\nabla\eta\,\mathrm{d}x - \int_\Omega \epsilon\nabla\phi^{n+1}\cdot\nabla u^n u^n\,\eta\mathrm{d}x$$
$$+\int_\Omega \frac{1}{\epsilon}G''(\phi^n)\phi^{n+1}\left(1-\frac{1}{2}(u^n)^2\right)\eta\,\mathrm{d}x + \int_\Omega \frac{1}{\epsilon}\left(G'(\phi^n)-G''(\phi^n)\phi^n\right)\left(1-\frac{1}{2}(u^n)^2\right)\eta\,\mathrm{d}x$$
$$-\int_\Omega u^n\eta\,\mathrm{d}x = 0.$$

This equation determines the geometry for a given adatom concentration. We then use the computed ϕ^{n+1} in the first equation to determine u^{n+1} by given u^n, ϕ^n and ϕ^{n+1}. Here we use a fully implicit time discretization

$$\int_\Omega \left(\frac{\epsilon}{2}|\nabla\phi^{n+1}|^2+\frac{1}{\epsilon}G(\phi^{n+1})\right)\frac{u^{n+1}-u^n}{\tau^n}\eta\,\mathrm{d}x + \int_\Omega \epsilon u^{n+1}\frac{\phi^{n+1}-\phi^n}{\tau^n}\nabla\phi^{n+1}\cdot\nabla\eta\,\mathrm{d}x$$
$$+\int_\Omega \epsilon u^{n+1}\frac{|\nabla\phi^{n+1}|^2}{\tau^n}\eta\,\mathrm{d}x - \int_\Omega \epsilon u^{n+1}\frac{\nabla\phi^{n+1}\cdot\nabla\phi^n}{\tau^n}\eta\,\mathrm{d}x + \int_\Omega \frac{1}{\epsilon}B(\phi^{n+1})\nabla u^{n+1}\cdot\nabla\eta\,\mathrm{d}x$$
$$+\int_\Omega \frac{1}{\epsilon}u^{n+1}G'(\phi^{n+1})\frac{\phi^{n+1}-\phi^n}{\tau^n}\eta\,\mathrm{d}x = \int_\Omega \frac{1}{\epsilon}B(\phi^{n+1})\boldsymbol{F}\frac{\nabla\phi^n}{|\nabla\phi^n|}\eta\,\mathrm{d}x - \int_\Omega \frac{\phi^{n+1}-\phi^n}{\tau^n}\eta\,\mathrm{d}x.$$

4.2. Finite element discretization

We discretize both equations in space by linear finite elements. Therefore, we let T_h^n be a conforming triangulation of Ω at t_m. We define the finite element space of globally continuous, piecewise linear elements $V_h^n = \{v_h \in X : v_h|_T \in P^1 \forall T \in T_h^n\}$, with $X = \{v \in H^1(\Omega) : v|_{\partial\Omega}$ periodic, or $v|_{\partial\Omega} = 0\}$ (see boundary conditions specified in sections 5.1 and 5.2). The space discretization now read

$$\int_\Omega \epsilon b \frac{\phi_h^{n+1}-\phi_h^n}{\tau^n}\eta\,\mathrm{d}x + \int_\Omega \epsilon\left(1-\frac{1}{2}(u_h^n)^2\right)\nabla\phi_h^{n+1}\cdot\nabla\eta\,\mathrm{d}x - \int_\Omega \epsilon\nabla\phi_h^{n+1}\cdot\nabla u_h^n u_h^n\eta\,\mathrm{d}x$$
$$+\int_\Omega \frac{1}{\epsilon}G''(\phi_h^n)\phi_h^{n+1}\left(1-\frac{1}{2}(u_h^n)^2\right)\eta\,\mathrm{d}x + \int_\Omega \frac{1}{\epsilon}\left(G'(\phi_h^n)-G''(\phi_h^n)\phi_h^n\right)\left(1-\frac{1}{2}(u_h^n)^2\right)\eta\,\mathrm{d}x$$
$$-\int_\Omega u_h^n\eta\,\mathrm{d}x = 0$$

and

$$\int_\Omega \left(\frac{\epsilon}{2}|\nabla\phi_h^{n+1}|^2+\frac{1}{\epsilon}G(\phi_h^{n+1})\right)\frac{u_h^{n+1}-u_h^n}{\tau^n}\eta\,\mathrm{d}x + \int_\Omega \epsilon u_h^{n+1}\frac{\phi_h^{n+1}-\phi_h^n}{\tau^n}\nabla\phi_h^{n+1}\cdot\nabla\eta\,\mathrm{d}x$$
$$+\int_\Omega \epsilon u_h^{n+1}\frac{|\nabla\phi_h^{n+1}|^2}{\tau^n}\eta\,\mathrm{d}x - \int_\Omega \epsilon u_h^{n+1}\frac{\nabla\phi_h^{n+1}\cdot\nabla\phi_h^n}{\tau^n}\eta\,\mathrm{d}x + \int_\Omega \frac{1}{\epsilon}B(\phi_h^{n+1})\nabla u_h^{n+1}\cdot\nabla\eta\,\mathrm{d}x$$
$$+\int_\Omega \frac{1}{\epsilon}u_h^{n+1}G'(\phi_h^{n+1})\frac{\phi_h^{n+1}-\phi_h^n}{\tau^n}\eta\,\mathrm{d}x = \int_\Omega \frac{1}{\epsilon}B(\phi_h^{n+1})\boldsymbol{F}\frac{\nabla\phi_h^{n+1}}{|\nabla\phi_h^{n+1}|}\eta\,\mathrm{d}x - \int_\Omega \frac{\phi_h^{n+1}-\phi_h^n}{\tau^n}\eta\,\mathrm{d}x$$

for all $\eta \in V_h^n$.

4.3. Linear systems of equations

The resulting systems for Φ^{n+1} and U^n, with $\phi_h^n = \sum \Phi_i^n \eta_i$ and $u_h^n = \sum U_i^n \eta_i$, are linear and of the form

$$\frac{1}{\tau^n}\epsilon b \boldsymbol{M}_1 \Phi^{n+1} + \epsilon \boldsymbol{A}_1 \Phi^{n+1} - \epsilon \boldsymbol{B}_1 \Phi^{n+1} + \frac{1}{\epsilon}\boldsymbol{C}_1 \Phi^{n+1} = \boldsymbol{F}_1 + \frac{1}{\tau^n}\epsilon b \boldsymbol{M}_1 \Phi^n$$

and

$$\frac{1}{\tau^n}\boldsymbol{M}_2 U^{n+1} + \epsilon \boldsymbol{B}_2 U^{n+1} + \epsilon \boldsymbol{C}_2 U^{n+1} + \frac{1}{\epsilon}\boldsymbol{A}_2 U^{n+1} = \boldsymbol{F}_2 + \frac{1}{\tau^n}\boldsymbol{M}_2 U^{n+1},$$

with

$$\begin{aligned}
&\boldsymbol{M}_1 = (M_{1,ij}),\ M_{1,ij} = (\eta_i, \eta_j)_\Omega \\
&\boldsymbol{A}_1 = (A_{1,ij}),\ A_{1,ij} = \left(\left(1 - \tfrac{1}{2}(u_h^n)^2\right)\nabla\eta_i, \nabla\eta_j\right)_\Omega \\
&\boldsymbol{B}_1 = (B_{1,ij}),\ B_{1,ij} = (\nabla\eta_i \cdot \nabla u_h^n u_h^n, \eta_j)_\Omega \\
&\boldsymbol{C}_1 = (C_{1,ij}),\ C_{1,ij} = \left(G''(\phi_h^n)\left(1 - \tfrac{1}{2}(u_h^n)^2\right)\eta_i, \eta_j\right)_\Omega \\
&\boldsymbol{F}_1 = (F_{1,i}),\ F_{1,i} = \left(-\frac{1}{\epsilon}(G'(\phi_h^n - G''(\phi_h^n))\left(1 - \tfrac{1}{2}(u_h^n)^2\right) + u_h^n, \eta_i\right)_\Omega
\end{aligned}$$

and

$$\boldsymbol{M}_2 = (M_{2,ij}),\ M_{2,ij} = \left(\left(\frac{\epsilon}{2}|\nabla\phi_h^{n+1}|^2 + \frac{1}{\epsilon}G(\phi_h^{n+1})\eta_i, \eta_j\right)\right)_\Omega$$

$$\boldsymbol{A}_2 = (A_{2,ij}),\ A_{2,ij} = (B(\phi_h^{n+1})\nabla\eta_i, \nabla\eta_j)_\Omega$$

$$\boldsymbol{B}_2 = (B_{2,ij}),\ B_{2,ij} = \left(\frac{\phi_h^{n+1} - \phi_h^n}{\tau^n}\nabla\phi_h^{n+1}\eta_i, \nabla\eta_j\right)_\Omega$$

$$\boldsymbol{C}_2 = (C_{2,ij}),\ C_{2,ij} = \left(\left(\frac{|\nabla\phi_h^{n+1}|^2}{\tau^n} - \frac{\nabla\phi_h^{n+1}\cdot\nabla\phi_h^n}{\tau^n} + \frac{1}{\epsilon^2}G'(\phi_h^{n+1})\frac{\phi_h^{n+1} - \phi_h^n}{\tau^n}\right)\eta_i, \eta_j\right)_\Omega$$

$$\boldsymbol{F}_2 = (F_{2,i}),\ F_{2,i} = \left(\frac{1}{\epsilon}B(\phi_h^{n+1})\boldsymbol{F}\frac{\nabla\phi_h^{n+1}}{|\nabla\phi_h^{n+1}|} - \frac{\phi_h^{n+1} - \phi_h^n}{\tau^n}, \eta_i\right)_\Omega,$$

where $(\cdot,\cdot)_\Omega$ denotes the L^2 scalar product. Both linear equations are solved by a conjugate gradient method.

4.4. Adaptivity

The problem to be solved is a fully two (three) dimensional problem. However the initial problem we are essentially interested in, the evolution of a curve (surface), is only one (two) dimensional. The additional dimension results from the simplicity to solve a partial differential equation on a time-independent Cartesian grid, and is the price we have to pay. Therefore to keep the computational cost comparable to a sharp interface front tracking code, even if such a code for this problem is not available at the moment, adaptivity is indispensable. Due to the high localization of the evolution at the diffuse interface the problem is also well suited for adaptive grid refinement and coarsening. Outside of the diffuse interface region the grid can be rather coarse, without influencing the solution on the surface. As a first approach towards an adaptive scheme we therefore choose a jump residual of the phase-field variable ϕ as an indicator, to refine and coarsen the mesh. The mesh is not modified according to the adatom concentration u, thus within the diffuse interface the mesh is uniform. See figure 1 for an example of an adaptively refined mesh.

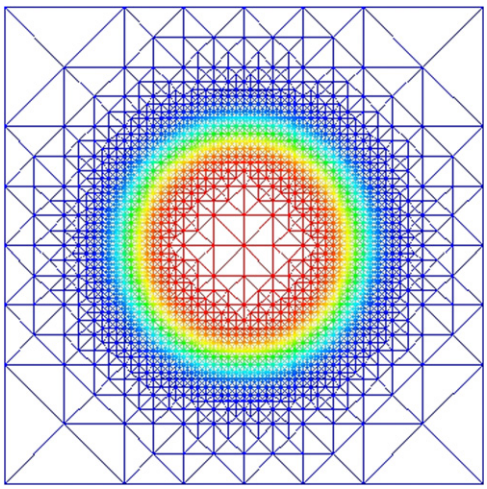

Figure 1. Adaptively refined mesh corresponding to a circular shape represented by the phase-field variable ϕ. The parameters in the error estimate are chosen such that the grid size within the diffuse interface is approximately $h_{\text{mesh}} \approx 0.2\epsilon$.

4.5. Implementation

The approach is implemented in AMDiS, an adaptive finite element toolbox for the efficient solution of systems of partial differential equations. For a description of the software and the algorithms implemented, see e.g. [18].

5. Numerical results

We now present some simulation results obtained with the scheme described above, which is modified at various points. To deal with the degeneracy of the equation we approximate $B(\phi^{n+1})$ by $B(\phi^{n+1}) + \delta$ in the second-order term, where δ is a small parameter. Such a numerical regularization has already been discussed in [16] and does not affect the asymptotic analysis. In the following simulations we chose $\epsilon = 2.5 \times 10^{-1}$ and $\delta = 1.0 \times 10^{-5}$. We further multiply the term $u^{n+1}\eta$ by $30(\phi^{n+1})^2(1-\phi^{n+1})^2$ to localize the influence. Again this modification does not influence the asymptotic analysis and is standard [11].

We start with a comparison with numerical results obtained within the graph formulation in [4] and then proceed to examples which cannot be represented by a graph.

5.1. Relaxation to planar curves

Consider the domain $\Omega = (-1, 1) \times (-1, 1)$ with periodic boundary conditions at the side walls and zero flux boundary conditions on top and bottom for u and ϕ. As initial conditions we use $u_0 = 0.2$ and $\phi_0 = 0.5(1 - \tanh(3(x_2 + 0.5 + 0.1\cos(x_1\pi))\epsilon^{-1}))$. For the kinetic coefficient we set $b = 1$ and the deposition flux is set to $\boldsymbol{F} = 0$. Figure 2 shows the interface corresponding to the 0.5-level set of ϕ and the adatom concentration on it at various times. After an initial adjustment of the adatom concentration the curve flattens and the adatom concentration adjusts to the velocity and the curvature. Afterwards, on a much slower time scale the adatom density decreases to zero on the flat interface. The results agree nicely with the computations in [4].

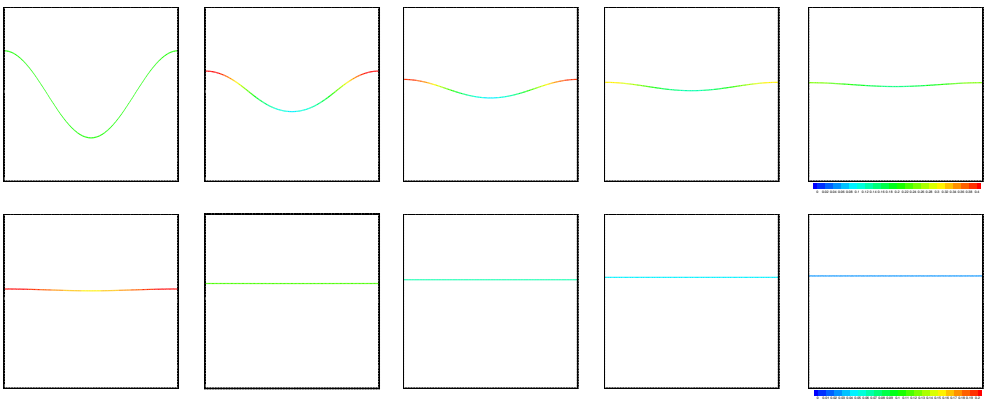

Figure 2. Adatom density on evolving curve at $t = 0.0, 0.1, 0.2, 0.3, 0.4$ (first row, colour bar from 0.0 to 0.4) and at $t = 0.5, 1.0, 1.5, 2.0, 2.5$ (second row, colour bar from 0.0 to 0.2). The time step is $\tau = 10^{-3}$.

5.2. Relaxation to circle

We now study closed curves Γ surrounding a domain $\Omega_{\text{in}} = \Omega_{\text{in}}(t) \subset \Omega$. If we consider an initial shape $\Omega_{\text{in}}(0)$ and a constant initial adatom concentration $u(0)$ on $\Gamma(0)$ the mass in the system is given by

$$m(0) = |\Omega_{\text{in}}(0)| + u(0)|\Gamma(0)|,$$

where $|\Omega_{\text{in}}|$ denotes the area of Ω_{in} and $|\Gamma|$ the length of Γ. The equilibrium shape should be circular and by (12) the adatom concentration constant; thus

$$m(t) = |\Omega_{\text{in}}(t)| + u(t)|\Gamma(t)|$$

for $t \to \infty$. In equilibrium ($V = 0$) we thus obtain from (13)

$$H - u - \tfrac{1}{2}u^2 H = 0.$$

All three equations, together with mass conservation

$$m(0) = m(t)$$

determine the curvature of the equilibrium circular shape and the constant adatom concentration on it, as a function of the initial values. For a circular initial shape with radius $R(0)$ we obtain

$$u_{\text{eq}} = \frac{1}{2}\sqrt{\frac{8}{3} - \frac{8}{3}R(0)^2 - \frac{16}{3}R(0)u(0) + 2\sqrt{\frac{16}{3} + \left(\frac{4}{3} - \frac{4}{3}R(0)^2 - \frac{8}{3}R(0)u(0)\right)^2}}.$$

As a first test case we start with a circle of radius $R(0) = 0.8$ and an initial adatom concentration of $u(0) = 0.825$, which approximately corresponds to the equilibrium configuration for R and u.

The corresponding initial condition for $\phi(0)$ thus reads $\phi(0) = 0.5(1 - \tanh(3(\|x\| - 0.8)\epsilon^{-1}))$ and $u(0) \equiv 0.825$ in the computational domain. Consider the domain $\Omega = (-1, 1) \times (-1, 1)$ with zero flux boundary conditions for u and ϕ. As expected ϕ and u remain almost constant in the simulation, see figure 3 and figure 4. The adjustment at the beginning results from the approximation of the stationary solution for ϕ through the used tanh-function. It should be noted that the variations in u are measured on Ω and not on Γ.

As a second test case we use a perturbed circular shape. Consider the domain $\Omega = (-2, 2) \times (-2, 2)$ with zero flux boundary conditions for u and ϕ. As initial conditions we

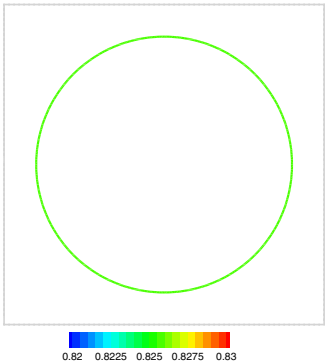

Figure 3. Adatom density on final curve at $t = 1.75$ (colour bar from 0.824 to 0.826).

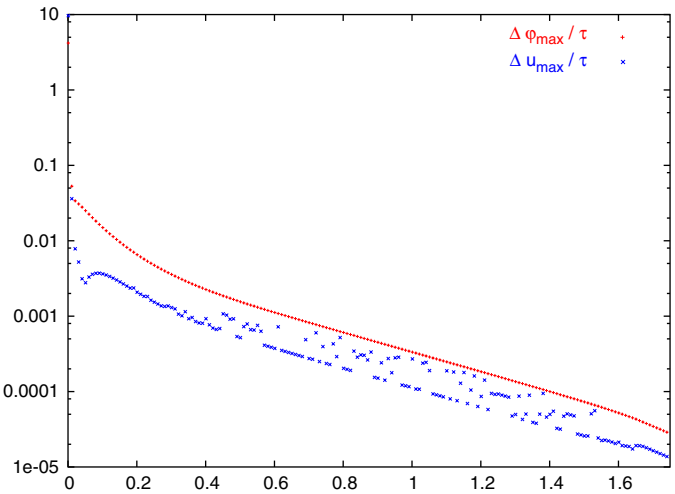

Figure 4. Maximal variation in ϕ and u in Ω over time. The time step is $\tau = 10^{-3}$. At $t = 1.75$ the prescribed solver tolerance is reached.

use $u_0 = 0.2$ and $\phi_0 = 0.5(1 - \tanh(3(\|x\| - 1.7 + 0.1\cos(4\theta))\epsilon^{-1}))$, where θ denotes the angle of x with the x_2-axis. For the kinetic coefficient we set $b = 1.0$ and the deposition flux is set to $\boldsymbol{F} = 0$. Figure 5 shows the interface corresponding to the 0.5 level set of ϕ and the adatom concentration on it at various times. The curve converges to a circle; during this evolution the adatom concentration adjusts to the local velocity and the local curvature. Afterwards on a much slower time scale the circle shrinks until the equilibrium shape is reached and the adatom concentration increases until the equilibrium concentration is reached. In contrast to the planar interface the adatom concentration does not decrease to zero, but evolves towards an equilibrium value, which is determined through the initial configuration. The final configuration is obtained through a compromise between minimizing the energy associated with curvature and minimizing the energy associated with the adatom concentration under the constraint of mass conservation.

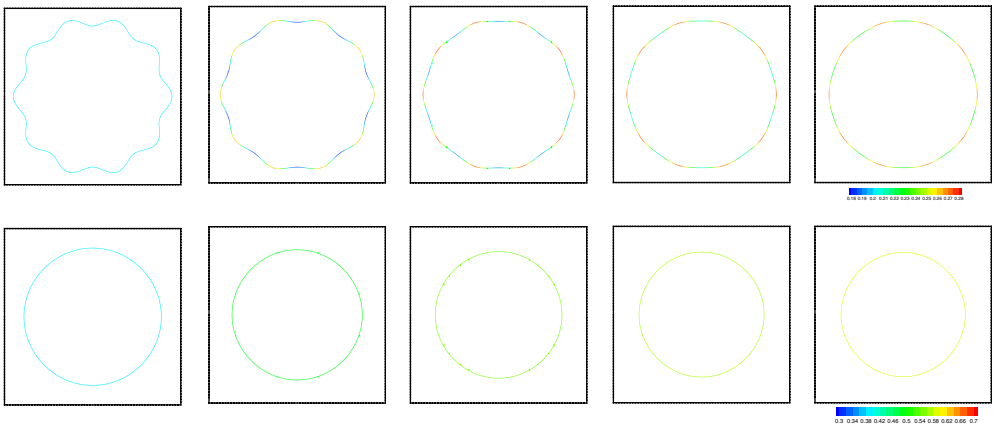

Figure 5. Adatom density on evolving curve at $t = 0.00, 0.02, 0.04, 0.06, 0.08$ (first row, colour bar from 0.18 to 0.28) and at $t = 0.5, 1.0, 1.5, 2.0, 2.5$ (second row, colour bar from 0.3 to 0.7). The time step is $\tau = 10^{-3}$. The final adatom density is 0.585 and the final radius is 1.409.

6. Conclusions

We presented a phase-field approximation for the problem of surface diffusion including adatoms. This problem can be interpreted as a diffusion equation on an evolving surface, where the evolution essentially is governed by mean curvature flow. The problem serves as a prototype for more general evolution equations on evolving surfaces and the prescribed phase-field approximation can easily be adapted to them. For an example where the evolution equation on the surface is of the Cahn–Hilliard type and the surface evolves by a modified Willmore flow, see, e.g. [12].

The numerical approach considered is based on a semi-implicit time discretization and a discretization in space by linear finite elements. Due to the higher dimensionality of the phase-field approach compared with the sharp interface description adaptivity is indispensable for the problem to keep the computational cost comparable to a sharp interface algorithm. Adaptivity in space is used in the simulations.

Simulations of the adatom surface diffusion model in a more realistic physical setting, with anisotropies in the surface free energy and kinetic coefficient, are the subject of ongoing work [17] and will be used to study thermal faceting and coarsening of growing surfaces.

Acknowledgments

The authors are grateful to Martin Burger for insightful discussions. AR and AV were supported by DFG through the SPP 'Analysis, Modeling and Simulation of multi-scale problems' under grant Vo 899/3-1, AV was further supported by EU FP6 through NMP STRP 016447 'MagDot'.

References

[1] Adalsteinsson D and Sethian J A 2003 Transport and diffusion of material quantities on propagating interfaces via level set methods *J. Comput. Phys.* **185** 271–88

[2] Alikakos N D, Bates P W and Chen X F 1994 Convergence of the Cahn–Hilliard equation to the Hele–Shaw model *Arch. Ration. Mech. Anal.* **128** 165–205
[3] Boettinger W J, Warren J A, Beckermann C and Karma A 2002 Phase-field simulation of solidification *Ann. Rev. Mater. Res.* **32** 163–94
[4] Burger M 2006 Surface diffusion including adatoms *Commun. Math. Sci.* **4** 1–51
[5] Cahn J W, Novick-Cohen A and Elliott C 1996 The Cahn–Hilliard equation with a concentration dependent mobility: motion by minus the Laplacian of the mean curvature *Eur. J. Appl. Math.* **7** 287–301
[6] Cahn J W and Taylor J E 1994 Surface motion by suface diffusion *Acta Metall. Mater.* **42** 1045–63
[7] Cermelli P, Fried E and Gurtin M E 2005 Transport relations for surface integrals arising in the formulation of balance laws for evolving fluid interfaces *J. Fluid Mech.* **544** 339–51
[8] Dziuk G and Elliott C 2006 Finite elements on evolving surfaces *IMA J. Numer. Anal.* at press
[9] Eggleston J J and Voorhees P W 2002 Ordered growth of nanocrystals via a morphological instability *Appl. Phys. Lett.* **80** 306–8
[10] Fried E and Gurtin M E 2004 A unified treatment of evolving interfaces accounting for small deformations and atomic transport with emphasis on grain-boundaries and epitaxy *Adv. Appl. Mech.* **40** 1–177
[11] Karma A and Rappel W J 1996 Phase-field method for computationally efficient modeling of solidification with arbitrary inteface kinetics *Phys. Rev.* E **53** R3017–20
[12] Lowengrub J S, Rätz A and Voigt A 2007 Phase seperation in biomembranes—a diffuse interface approach, in preparation
[13] Mullins W W 1957 Theory of thermal grooving *J. Appl. Phys.* **28** 333–9
[14] Pego R L 1989 Front migration in the nonlinear Cahn–Hilliard equation *Proc. R. Soc. Lond.* A **422** 261–78
[15] Rätz A, Ribalta A and Voigt A 2006 Surface evolution of elastically stressed films under deposition by a diffuse interface model *J. Comput. Phys.* **214** 187–208
[16] Rätz A and Voigt A 2006 PDE's on surfaces—a diffuse interface approach *Commun. Math. Sci.* **4** 3436–45
[17] Stöcker C and Voigt A A level set approach to anisotropic surface evolution with free adatoms *Technical Report* in preparation
[18] Vey S and Voigt A 2007 AMDiS—adaptive multidimensional simulations *Comput. Vis. Sci.* at press
[19] Wise S M, Lowengrub J S, Kim J S, Thornton K, Voorhees P W and Johnson W C 2005 Quantum dot formation on a strain-patterned epitaxial thin film *Appl. Phys. Lett.* **87** 133102
[20] Xu J J and Zhao H K 2003 An Eulerian formulation for solving partial differential equations along a moving interface *J. Sci. Comput.* **19** 573–94